

Supramolecular photochemistry of drugs in biomolecular environments

Cite this: DOI: 10.1039/c3cs60402k

Sandra Monti and Ilse Manet

In this tutorial review we illustrate how the interaction of photoactive drugs/potential drugs with proteins or DNA in supramolecular complexes can determine the course of the reactions initiated by the drug absorbed photons, evidencing the mechanistic differences with respect to the solution conditions. We focus on photoprocesses, independent of oxygen, that lead to chemical modification of the biomolecules, with formation of new covalent bonds or cleavage of existing bonds. Representative systems are mainly selected from the literature of the last decade. The photoreactivity of some aryl propionic acids, (fluoro)quinolones, furocoumarins, metal coordination complexes, quinine-like compounds, naphthaleneimides and pyrenyl-peptides with proteins or DNA is discussed. The use of light for biomolecule photomodification, historically relevant to biological photosensitization processes and some forms of photochemotherapy, is nowadays becoming more and more important in the development of innovative methods in nanomedicine and biotechnology.

Received 7th November 2013

DOI: 10.1039/c3cs60402k

www.rsc.org/csr

Key learning points

The main mechanisms of photochemical modification of proteins and DNA, with formation of new covalent bonds or cleavage of existing bonds, induced by drugs absorbing light in drug–biomolecule supramolecular complexes.

The importance of the drug affinity for biomolecules in a study targeting the comprehension of the drug photochemistry in the presence of biomolecules.

The control of the final photochemical outcome *via* the supramolecular architecture of the drug–biomolecule complex.

The advantage of using light as a reagent for biomolecule modification in mild reaction conditions.

Supramolecular drug photochemistry as an inspiration source for innovation in nanomedicine.

1. Introduction

During the last few decades a lot of basic research has been focused on the photochemistry of drugs in homogeneous solution and in systems mimicking a biological environment.^{1–5} This research was driven by the need to understand and control drug-induced phototoxicity and photoallergy during treatment,⁶ but also inspired scientists looking for innovative photochemotherapies. Indeed therapeutic approaches based on drugs activatable by light have attracted interest and have been developed more and more playing a marginal, but significant role in clinical practice. Regulation of the therapeutic action of a drug exclusively at the target site represents a very appealing goal. Light as an activating agent has a number of advantages over other regulating methods, because irradiation can be easily controlled in space and time, thereby confining drug activity to selected tissues with negligible side effects.⁷

The photobiological activity relies on photon absorption by the drug, generally embedded in a biomolecular matrix, and on *in situ* generation of reactive intermediates. These species can either diffuse away, randomly attacking “distant” targets, or react specifically with substrates in the immediate vicinity of the production site, causing a “local” chemical modification. The first case is that of photosensitized production of singlet oxygen, superoxide anion or nitric oxide, whereas the second one is that of covalent photobinding, photoalkylation, photocrosslinking and site-selective photocleavage of proteins and nucleic acids.

In this research frame it is mandatory to have thorough knowledge of the photoreactivity of the drug in conditions similar, as much as possible, to those of the biological system. Indeed the nature of the interactions and the molecular species close to the drug in the binding site critically determine the fate of the excited drug and the photochemically generated intermediates. In this tutorial review we want to highlight how a biomolecular matrix can actually determine the course of the reactions initiated by a photoexcited drug, evidencing the differences with respect to the solution conditions. This is

Istituto per la Sintesi Organica e la Fotoreattività, CNR, via Gobetti 101, 40129 Bologna, Italy. E-mail: sandra.monti@isof.cnr.it

1 performed through the illustration of the photoreactivity of
some selected drugs or drug candidates (in the following
named “drugs” for the sake of simplicity), when complexed
to protein and DNA. Representative examples are taken mainly
5 from the literature of the last decade.

2. Photoexcitation of drugs and deactivation processes in biomolecular complexes

10 Upon photon absorption a drug in solution is promoted to an
excited state and can lose its excess energy by the release of heat
to the medium, emission of a photon of different energy or
15 participation in chemical processes. The lowest singlet and
triplet excited states are generally the starting point for emis-
sion of photons and chemical reactions. While the emission
process leaves the drug unaltered, participation in a chemical
reaction can have different outcomes, depending on whether
20 the drug acts as an individual entity undergoing intramolecu-
lar photochemistry or is involved in intermolecular reactions with
other species in close proximity. Basically three types of inter-
molecular processes can be discerned in the chemical evolution
of the excited drug. Type I processes involve radical species
25 formed upon interaction of the excited drug with a substrate,
like oxygen or biomolecules, participating in charge transfer or
H-abstraction;⁸ type II processes involve formation of singlet
oxygen upon triplet energy transfer to molecular oxygen; type III
processes generally refer to reactions of the excited state with a
30 substrate “directly” giving products and may be mediated by

energy transfer processes.^{4,8–10} Intramolecular reactions like
the photorelease of a fragment can generate reactive intermedi-
ates ascribed to the type I class.^{2,3,11}

5 In a drug–biomolecule complex the deactivation paths of the
excited drug can be markedly different from those of the drug
in solution and be influenced by several factors, including the
hydrophobicity of the binding site, the steric constraints
imposed by the complex geometry, the proton-, electron- or
10 H-donating ability of the neighboring molecular species, and
the shielding action exerted by the environment. Due to the
close vicinity of the drug and biomolecule in the complex, the
chemical reactions may be much faster than in solution with-
out the need for any diffusion for partner encounter. Obviously
15 this vicinity changes drastically also the conditions for compe-
tition of other actors, like for example oxygen, able to quench
diffusively the excited drug. When studying the photochemical
behaviour of a drug–biomolecule complex, knowledge of the
drug photochemistry in the homogeneous buffer is a prerequi-
20 site. A next step commonly consists in the study of the photo-
chemical behaviour of the drug in the presence of simple
models like single amino acids and nucleotides. Eventually
the drug photochemistry is studied in the supramolecular
complex. The literature dealing with drug photochemistry in
the presence of biomolecules or their models is huge; however
25 very often essential information is missing on the partition
between free and complexed drug in the system. Indeed in the
presence of a certain amount of free drug the discernment of
the photoprocesses occurring in the complex ends up being
much more complicated. Therefore a careful study of the drug
30 affinity for the biomolecule concomitant to the investigation of



Sandra Monti

Sandra Monti is Doctor in Physics. She carried out postdoctoral research and joined CNR at the Institute of Biophysics of the Italian National Research Council (CNR) in Pisa (Italy). Then she moved to the Institute for the Organic Synthesis and Photoreactivity (ISOF) in Bologna (Italy), conducting research as Senior Scientist until 2011 and then as Associate Scientist. She served as President of the Italian Group of

Photochemistry and member of the Ownership Board of Photochemical and Photobiological Sciences (PPS) of RSC. She is a member of the PPS Editorial Board since 2002. Her scientific interests span the fields of physical chemistry and photochemistry of organic molecules with a focus on supramolecular photochemistry and photophysics of drugs non-covalently bound to artificial carriers and biomolecules. Methods of investigation involve optical absorption, circular dichroism and fluorescence and detection of intermediates using time resolved techniques.



Ilse Manet

Ilse Manet graduated in Chemistry at the Catholic University of Leuven in 1992 and in 1998 she received her PhD degree in Chemical Sciences from the University of Bologna studying luminescent supramolecular systems acting as antennas and sensors. Since 2001 she is a permanent researcher at the Istituto per la Sintesi Organica e la Fotoreattività (ISOF). Her research focuses on different topics: non-covalent interactions

in ligand–receptor systems of biological and pharmacological interest studied with different spectroscopic optical techniques in both steady-state and time-resolved modality; photoreactivity of drugs in solution and complexed to a biological substrate. Recently she started working in the field of laser scanning confocal fluorescence microscopy implementing time-resolved fluorescence imaging for materials study and cellular drug delivery.

1 photochemistry in the complex is necessary. Several analytical
 2 techniques are available to study the affinity of a drug for a
 3 biomolecule, among which isothermal titration calorimetry,
 4 surface plasmon resonance, mass spectrometry and UV-Vis
 5 spectroscopic techniques (absorption, circular dichroism,
 6 fluorescence) are most frequently encountered. Time-resolved
 7 techniques (absorption or resonance Raman) afford precious
 8 information on the transient intermediates generated photo-
 9 chemically. The UV-Vis absorption fingerprints of radicals of
 10 single amino acids and nucleotides help interpretation of the
 11 time-resolved absorption spectra obtained for the complex.
 12 Several trapping agents specific for reactive intermediates offer
 13 a precious tool to understand the nature of the transients.
 14 Steady state irradiation of the complex in different experi-
 15 mental conditions, such as aerobic and anaerobic, with and
 16 without selective traps, generates photoproducts to be analysed
 17 subsequently. The analytical techniques can vary if focus is on
 18 the drug photoproduct or on the photochemically modified
 19 biomolecule or on both.

20 Keeping in mind the concepts outlined in this section we
 21 will discuss next some examples of drug photochemistry in the
 22 presence of biomolecules with particular attention on systems
 23 where the drug binding conditions are known. Focusing on
 24 events in drug–biomolecule complexes implies that photoreac-
 25 tions requiring diffusional encounter of the participating spe-
 26 cies will be only marginally treated. We will divide the drug
 27 photosensitized processes into two categories: photoinduced
 28 formation of new covalent bonds and cleavage of existing
 29 bonds in the biomolecule.

3. Drug photosensitized formation of new covalent bonds

3.1. Proteins

35 It is generally accepted that light driven formation of covalent
 36 adducts of drugs and proteins is the primary step of drug-
 37 induced photoallergic manifestations.⁶ The modified protein
 38 represents an antigen for the immune system which reacts with
 39 a hypersensitivity delayed response. Among the families of
 40 photosensitizing drugs known to cause this type of disorder
 41 the nonsteroidal anti-inflammatory drugs (NSAID) and the
 42 antibacterial fluoroquinolones have been more deeply studied.
 43 Drug–protein interaction in solution has been studied mostly
 44 with serum albumins (SAs). SAs are devoted to transport of
 45 exogenous and endogenous compounds by the bloodstream.
 46 Human serum albumin (HSA) is a monomeric peptide of 66
 47 kDa containing 585 amino acids, among which there are 31
 48 phenylalanines (Phe), 18 tyrosines (Tyr) and 1 tryptophan (Trp)
 49 as aromatic amino acids. The crystal structure of HSA shows a
 50 heart-shaped protein with three homologous domains, I, II,
 51 and III, each divided into two subdomains, A and B, stabilized
 52 by 17 disulphide bridges and each endowed with 10 helical tracts
 53 (Fig. 1).¹² Medium size hydrophobic aromatics and heterocycles
 54 preferentially bind two sites located in subdomains IIA and IIIA,
 55 identified as Sudlow I and II sites, respectively. Additional binding

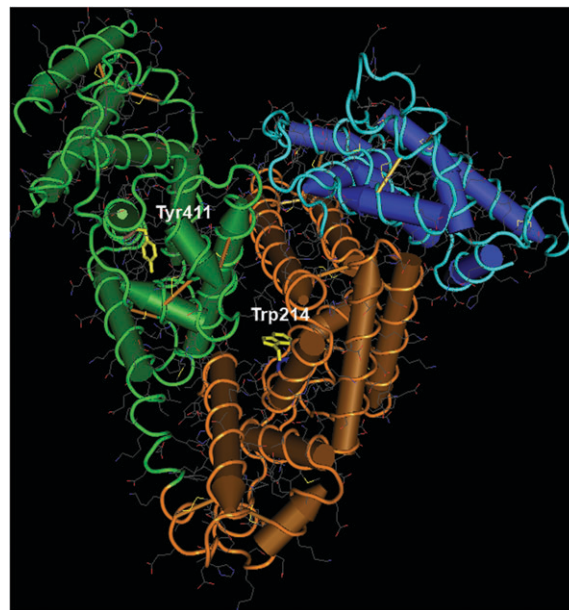
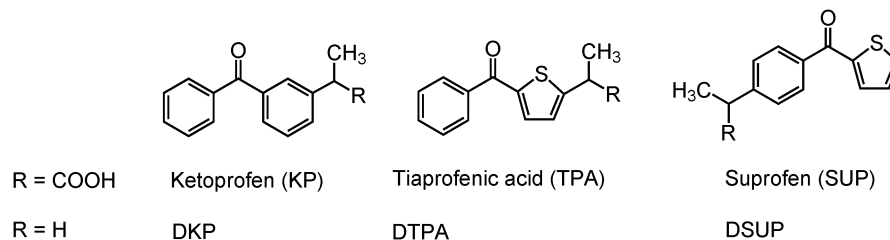


Fig. 1 Cartoon of HSA (obtained from the structure with PDB code 1AO6); domain I is blue, domain II is brown and domain III is green, Tyr 411 and Trp214 are evidenced. Reprinted with permission from ref. 32. Copyright (2008) American Chemical Society.

56 sites have been assigned to small size drugs and long chain fatty
 57 acids. In the main sites (I and II) two aromatic residues play a key
 58 role: Trp 214 in subdomain IIA with a relatively hydrophilic
 59 environment and Tyr411 in subdomain IIIA in a more hydro-
 60 phobic pocket. Bovine serum albumin (BSA) is also used as a
 61 model for binding studies even though no crystal structure is
 62 available. This protein has 76% sequence homology with HSA
 63 and lower local flexibility resulting in better selectivity in the
 64 stereochemical recognition of guests. Noticeably it has two
 65 tryptophan residues: Trp 212 in subdomain IIA and Trp 134 in
 66 subdomain IA.¹²

3.1.1 Benzophenone-like drugs. Non-steroidal anti-inflammatory
 67 drugs (NSAID) represent one of the most widely investigated
 68 classes of drugs as regards the mechanisms of protein covalent
 69 photobinding. In particular the aryl propionic acids containing
 70 benzophenone (BP) or benzoylthiophene moieties, like ketoprofen
 71 (KP), tiaprofenic acid (TPA), and suprofen (SUP) (Scheme 1),
 72 have been thoroughly studied as regards spectroscopic and
 73 photochemical properties in neutral aqueous buffer and other
 74 media including SA, for which they show high affinity ($K_{\text{ass}} \approx 10^5$ – 10^6
 75 M^{-1}).^{13–15} In spite of structural analogies, the character and
 76 energetic layout of their electronic states strongly depend on the
 77 nature of the aryl groups. KP in neutral aqueous buffer has an
 78 absorption band with a maximum at 260 nm ($\epsilon_{\text{max}} \sim 1.6 \times 10^4$
 79 $\text{M}^{-1} \text{cm}^{-1}$), similar to that of BP, attributed to the $S_0 \rightarrow S_2$
 80 transition of π, π^* character with a shoulder in the 300–350 nm
 81 region ($\epsilon_{\text{max}} \approx 10^2 \text{M}^{-1} \text{cm}^{-1}$) corresponding to the $S_0 \rightarrow S_1$
 82 forbidden transition of n, π^* character. Very efficient ISC popu-
 83 lates the lowest triplet T_1 (n, π^* , see below) making the mole-
 84 cule non-fluorescent. On the other hand the absorption spectra
 85 of TPA and SUP are



Scheme 1 Examples of aryl propionic acids containing a benzophenone or benzoylthiophene moiety.

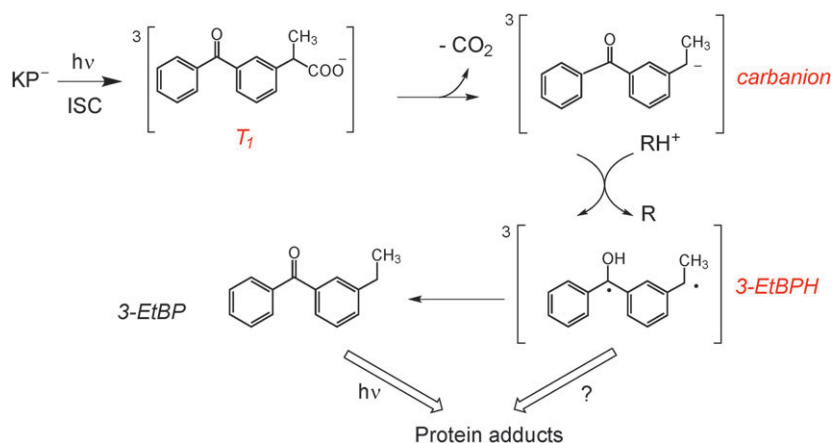
characterized by π,π^* bands with a maximum at 314 nm and 300 nm ($\epsilon_{\max} \sim 1.4 \times 10^4 \text{ M}^{-1} \text{ cm}^{-1}$) both endowed with intense shoulders at 266 nm ($\epsilon_{\max} \sim 0.8 \times 10^4 \text{ M}^{-1} \text{ cm}^{-1}$) and 270 nm ($1.25 \times 10^4 \text{ M}^{-1}$), respectively. A weak absorption tail extends beyond 360 nm for both benzoylthiophene-like molecules. It is assigned to the $S_0 \rightarrow S_1$ transition of n,π^* parentage, with sizeable absorption coefficients due to the distortion of the thiophene ring. TPA and SUP are weakly fluorescent. Another important difference of TPA and SUP compared to KP is the π,π^* character of the lowest triplet T_1 with microsecond lifetime and an energy gap from T_2 (n,π^*) of 15 and $\sim 11 \text{ kcal mol}^{-1}$, respectively, on the basis of ZINDO/S calculations. UVA excited drugs in their anionic form in neutral aqueous media (indicated in the following as TPA^- , SUP^- , KP^-) undergo efficient decarboxylation ($\Phi_{-\text{CO}_2} \approx 0.25\text{--}0.75$ at 20°C) leading to the corresponding photoproducts (Scheme 1).³ The latter maintain the photoactive chromophore and may act as even more efficient photosensitizing agents.¹⁶ Noticeably the photodecarboxylation mechanism critically depends on the molecular structure and the environment. Indeed change of medium from aqueous buffer to the hydrophobic β -cyclodextrin cavity affects the photoreactivity in a different way in the three drugs. The photodecomposition of KP is practically unaffected while that of both benzoylthiophene drugs is enhanced.

Irradiation of TPA in the presence of BSA, with a large molar excess of drug, preferentially damages the residues histidine (His), Tyr, and Trp and generates covalent drug–protein adducts as well as protein photocrosslinks.¹⁷ The benzoylthiophene triplet detected by laser flash photolysis is the starting point for both type I and type II processes. His is oxidized by singlet oxygen in type II processes, Trp participates in both type I and type II reactions, and Tyr is mainly degraded in type I processes. SUP and KP induce analogous modifications in the SA matrix.⁵ Tyr has been indicated to be involved in the formation of photoadducts. Full structural characterization of the adducts has not been achieved, but the use of highly specific antibodies to drug chemical epitopes has allowed discrimination between the different modes by which TPA, SUP and KP photobind to BSA, evidencing that the binding geometry critically depends on the drug molecular structure.⁵ It was concluded that TPA binds preferentially *via* the thiophene ring, and SUP and KP *via* the propionic acid-substituted benzene ring. Photobound TPA and KP substructures are recognized through the benzoyl moiety providing a rationale for the immunological cross-reactivity to TPA and KP observed in clinical studies.¹⁸

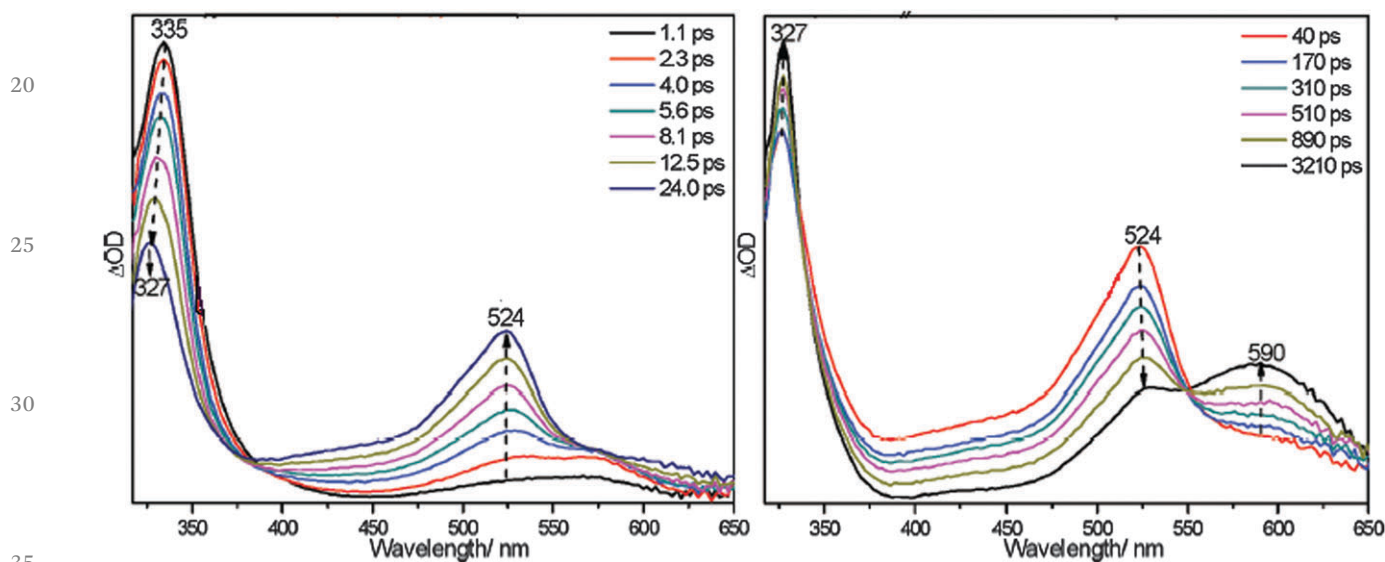
A difference in photosensitizing power is observed for KP, TPA and SUP in cell cultures, with the benzoylthiophenes more effective than KP. This mainly relates to the absorption coefficients in the UVA region, much larger for the TPA and SUP than for KP, and to the lifetime of the lowest triplet state, crucial for the overall drug photoreactivity, much longer in TPA and SUP than in KP. This will be illustrated in the following section on the photochemistry of these drugs, evidencing when possible the role of a protein matrix in the fate of excited states and intermediates.

The KP photochemistry in homogeneous buffer as well as in SA complexes represents a useful starting point. The photodecomposition quantum yield of KP^- depends on the environment: it does not show appreciable variation from neutral phosphate buffer (PB) to a cyclodextrin cavity¹⁹ or the HSA matrix,¹⁵ but decreases significantly in the BSA matrix.¹⁴ The main photoproduct in the absence of oxygen is in all cases 3-ethylbenzophenone (3-EtBP). As to the reactive excited state, its spin multiplicity in neutral buffer has been the object of debate,^{3,20} but has been recently ascertained to be the lowest triplet.²¹ The reaction mechanism is summarized in Scheme 2.

Femtosecond transient absorption (fs-TA) in 1:1 MeCN:PB saline (PBS) solution clearly evidences the benzophenone-like n,π^* lowest triplet (band with $\lambda_{\max} = 524 \text{ nm}$, Fig. 2, left) converting with a time constant of a few hundreds of picoseconds into a species with $\lambda_{\max} = 590 \text{ nm}$ (Fig. 2, right) assigned to the decarboxylated triplet carbanion intermediate on the basis of nanosecond time resolved resonance Raman spectra (ns-TR³).²¹ The carbanion at neutral pH undergoes protonation with a pseudo-first order rate constant $k \approx 10^7 \text{ s}^{-1}$ to form a longlived neutral triplet biradical ($\lambda_{\max} = 525 \text{ nm}$, lifetime of a few microseconds).^{3,22} The decays of initial triplet and triplet carbanion are both controlled by the environment. The rate of the photodecarboxylation process determines the lifetime of the KP triplet state, *ca.* 250 ps in buffer, but much longer in constrained, hydrophobic pockets like the cavity of β -cyclodextrin (*ca.* 50–100 ns)¹⁹ or the BSA and HSA binding sites (several hundreds of ns).^{14,15} The rate of protonation determines the lifetime of the carbanion, which in the β -cyclodextrin complex is longer lived than in PB.¹⁹ This intermediate is not at all detected in the protein complexes, even though photodecarboxylation remains the main reaction.^{14,15} The triplet neutral biradical is an intrinsically longlived intermediate, that in neutral buffer converts to 3-ethylbenzophenone (3-EtBP) presumably *via* intersystem crossing (ISC) and H-migration (likely mediated by solvent).



15 **Scheme 2** Mechanism proposed for the photodecomposition of KP^- in neutral PB saline (PBS) buffer and in the presence of a protein.



35 **Fig. 2** Femtosecond transient absorption spectra of KP^- in MeCN:PBS 1:1 solution at different delay times after the laser pulse; adapted with permission from ref. 21. Copyright (2012) American Chemical Society.

40 Protonated amino acids like histidine (HisH^+), lysine (LysH^+) and arginine (ArgH^+), as well as Tyr and Trp, substantially accelerate the carbanion protonation at neutral pH. Specific bimolecular rate constants for the conversion of the carbanion to the neutral biradical are $k_r = 4.6 \times 10^9 \text{ M}^{-1} \text{ s}^{-1}$ for His, $1.2\text{--}1.3 \times 10^8 \text{ M}^{-1} \text{ s}^{-1}$ for Lys and Arg, and $2.7 \times 10^9 \text{ M}^{-1} \text{ s}^{-1}$ and $7.8 \times 10^8 \text{ M}^{-1} \text{ s}^{-1}$, respectively, for Trp and Tyr.²³

45 As mentioned, nanosecond transient absorption spectra of the KP -SA diastereoisomeric complexes did not evidence the absorption band at 590 nm typical of the carbanion. Instead two transients were detected having different lifetimes of several hundreds of nanoseconds and a few microseconds and similar absorption spectra with $\lambda_{\text{max}} = 525\text{--}530 \text{ nm}$. With some caution the shorter lived transient was assigned to the KP^- triplet and the longer lived one to the decarboxylated triplet biradical, on the basis of the absorption features only.^{14,15} Nevertheless fast formation of the neutral biradical in the protein matrix is likely considering the structural

40 features of the SA complexes. Combination of fluorescence, molecular modelling and circular dichroism data provided the binding geometry of the KP enantiomers in the BSA matrix.²⁴ In both subdomains IIIA and IIA they closely interact *via* the negatively charged carboxylate group with positively charged or polarisable groups of the protein. In particular, Tyr409, Arg411, Thr410, Arg 408, Arg483 and Thr447 in subdomain IIIA and Trp212, His240, Arg216, Arg255 and Lys220 in subdomain IIA lie at short distances from either KP enantiomer (see as example the IIIA binding geometry in Fig. 3). Given the high rate constant k_r of the protonation of the carbanion intermediate by some of these amino acids in solution, the latter is reasonably not allowed to accumulate in the KP -protein complexes, the neutral biradical “directly forming” on the nanosecond time scale. Product analysis has shown that the covalent photobinding of KP to HSA occurs at Arg 485.²⁵ Noticeably, Arg483, the corresponding residue in BSA, is one of those in close proximity of the drug in the complex

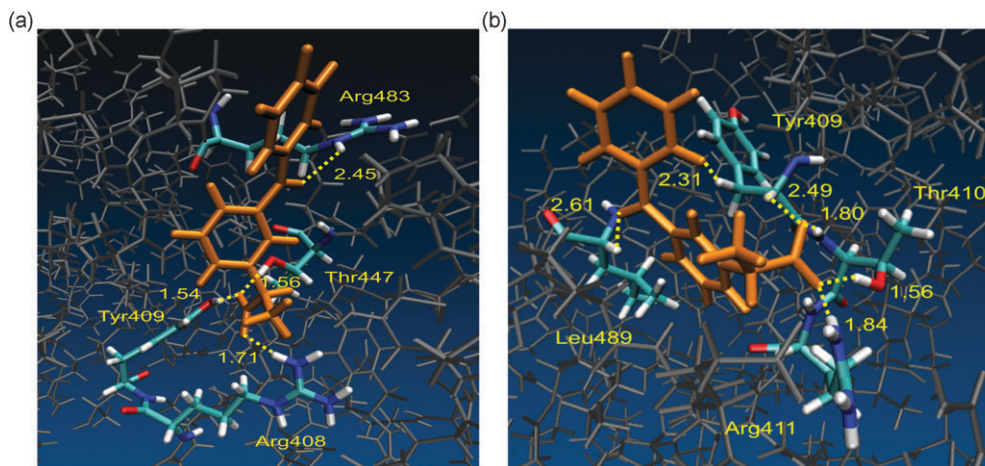


Fig. 3 Calculated structure of (a) R(-)-KP and (b) S(+)-KP, docked in BSA subdomain IIIA; reproduced from ref. 24 with permission from The Royal Society of Chemistry.

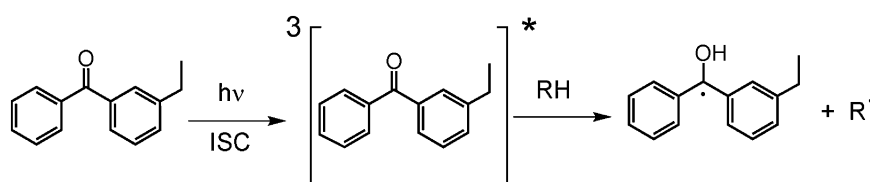
(see structure (a) in Fig. 3). As to the mechanism by which the eventual covalent bond can form, it could be argued that the triplet neutral biradical in the protein environment undergoes reaction with the closely lying arginine residue, finally leading to the chemical modification of the biomolecule. However no proof of this mechanism has yet been achieved.

TPA⁻ and SUP⁻ photodecomposition with light of $\lambda > 337$ nm in neutral PB is a thermally activated process (ΔE ca. 9–10 kcal mol⁻¹). Laser flash photolysis at 355 nm suggests that photodecarboxylation does not proceed from the lowest triplet (π, π^* character, μ s lifetime) but from an upper triplet (likely T₂ n, π^*) not accessible to direct observation. The path to the final photoproducts involves triplet carbanion and biradical intermediates analogous to those formed in the KP photodecarboxylation process. When TPA⁻ and SUP⁻ are embedded in the β -cyclodextrin cavity, the activation energy of the photo-reaction decreases by ca. 4–5 kcal mol⁻¹, making photodecomposition more efficient than in aqueous medium.³ The photodecarboxylation of TPA⁻ has been very recently explored with excitation at 267 or 266 nm by femto- and nanosecond transient absorption and nanosecond TR³ in neutral PBS:MeCN 7:3 mixtures and a different mechanism has been proposed.²⁶ The authors identified the lowest triplet of n, π^* character as the photoreactive state on the basis of DFT calculations and assigned a 320 ps time constant to the release of the CO₂ fragment and a 152 ns time constant to the protonation of the triplet carbanion. No temperature dependence has been studied. The different medium and excitation wavelengths make

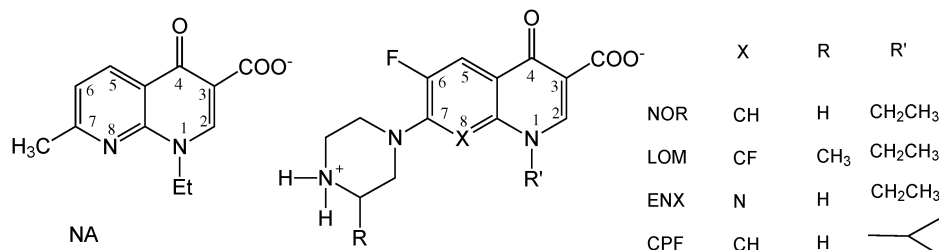
comparison of recent results with early ones difficult. No mechanistic studies have been carried out on the photodecarboxylation process in TPA and SUP within serum albumin.

As we have anticipated, strong candidates for producing the photoadducts to proteins are also the decarboxylated photo-products of TPA⁻, SUP⁻, and KP⁻, much more hydrophobic than the parent molecules and expected to remain strongly associated with the protein frame upon their formation. These products, accumulating in the system, can efficiently induce damage by secondary photochemistry. If excited to their long-lived benzophenone-like triplet, they can abstract hydrogen (Scheme 3) or accept one electron (and one proton) from a protein amino acid. The ensuing radical pair can easily generate the photoadduct upon radical–radical combination. Secondary photochemistry leading to covalent addition of 3-EtBP to β -cyclodextrin has been actually demonstrated by means of mass spectrometry upon irradiation of KP- β -cyclodextrin diastereoisomeric complexes.¹⁹ Because of the differences in the photochemical properties of TPA, SUP, and KP, secondary photochemistry is expected to play a role to a different extent in photosensitization processes.

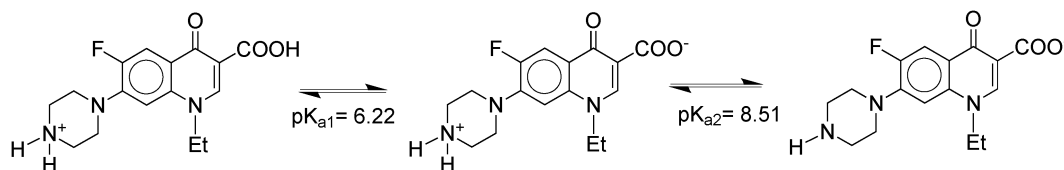
3.1.2 Fluoroquinolones and the case of nalidixic acid–serum albumin complexes. Quinolone-like drugs are antibacterial agents with inhibitory activity on bacterial topoisomerase of both Gram-positive and Gram-negative organisms. Referring to some representative structures in Scheme 4, we distinguish a non-fluorinated old member of the family, nalidixic acid (NA), and the next generation fluoroquinolones (FQs) with a broader



Scheme 3 Triplet photoreactivity of 3-EtBP.



Scheme 4 Nalidixic acid (NA), norfloxacin (NOR), lomefloxacin (LOM), enoxacin (ENX) and cyprofloxacin (CPF) forms present in neutral aqueous medium.



Scheme 5 Ionization equilibria of norfloxacin.

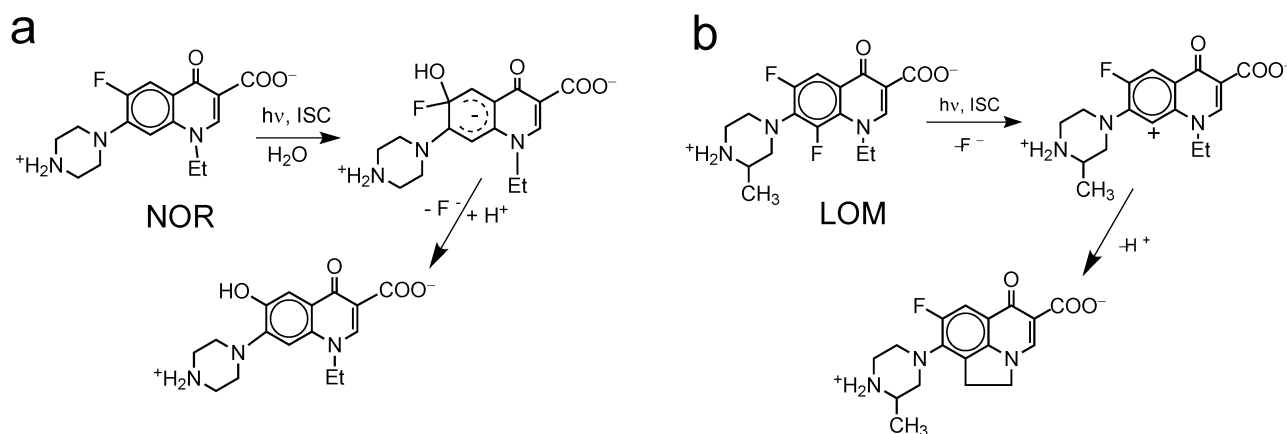
spectrum of activity, containing a piperazinyl substituent at C7 and either a single fluorine atom at C6 or two fluorine atoms at C6 and C8 in the quinolone nucleus, as key structural features. These molecules are all able to produce severe phototoxic and photoallergic effects.²⁷

The spectroscopic and photophysical properties of fluoroquinolones (FQ) have been reviewed and some relevant aspects are recalled here.² Due to the carboxylic group and the 4'-amino group of the piperazinyl ring two protonation equilibria are present, with pK_{a1} in the range 5.5–6.2 and pK_{a2} in the range 7.8–8.5, respectively (Scheme 5).

At neutral pH the largely prevailing species is the zwitterion, characterized by an absorption band with a maximum in the 260–300 nm region and a molar absorption coefficient, ϵ_{\max} , of $\approx 2.0\text{--}2.5 \times 10^4 \text{ M}^{-1} \text{ cm}^{-1}$, a band centered at 320–340 nm with ϵ_{\max} of $\approx 10^4 \text{ M}^{-1} \text{ cm}^{-1}$ and a weak tail extending beyond 350 nm. Fluorescence is significant for zwitterionic and cationic forms and poor for the anions. The emission spectra of the zwitterions are broad and structureless and exhibit large Stokes

shifts, consistent with a different geometry of the emitting state with respect to the ground state, associated to a large change in the dipole moment. The fluorescence quantum yields are generally around 10%. The fluorescence lifetimes are rather short (for example, $\sim 1.5 \text{ ns}$ for NOR and $\leq 1 \text{ ns}$ for LOM and ENX). The lowest triplet states at 260–280 kJ mol^{-1} energy are typically populated with good ISC yields and decay in the microsecond domain for 6-monofluoro derivatives and in the nanosecond domain for 6,8-difluoro derivatives.^{2,28,29}

The excited state reactions strongly depend on the molecular structure and the characteristics of the medium.² Typically, 6-monofluoro derivatives undergo photosubstitution at C6 *via* their longlived triplet state and a cyclohexadienyl anion (Scheme 6a), whereas 6,8-difluoro derivatives undergo photo-defluorination in position C8 *via* the shortlived triplet with the formation of an aryl cation which reacts intramolecularly (Scheme 6b). Nanosecond flash photolysis of LOM at 355 nm revealed the involved transients: a short-lived species ($\lambda_{\max} = 370 \text{ nm}$, $\tau_T = 40 \text{ ns}$) assigned to ^3LOM , and a further transient

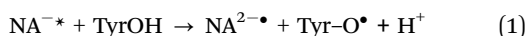


Scheme 6 Main photoreactions outlined for (a) NOR and (b) LOM in neutral aqueous medium.

1 identified as the triplet aryl cation ${}^3\text{AC}^+$ ($\lambda_{\text{max}} = 480 \text{ nm}$, $\tau = 120$
 ns),²⁸ which by intramolecular hydrogen abstraction from the
 N-ethyl chain gives the cyclization product. Other authors
 assigned these transients to the aryl cation in a triplet-singlet
 5 equilibrium.³⁰ Degradation quantum yields strongly depend on
 the chemical structure of the FQ, decreasing from LOM (0.55) to
 ENX (0.13) and NOR (0.06) in deoxygenated neutral aqueous
 medium. Other photoprocesses like decarboxylations and side
 chain degradation have been observed.

10 Some information on the possible mechanism for the forma-
 tion of FQ-protein photoadducts was recently obtained with
 the identification of the transients generated with some 6-F-
 quinolones, excited in the presence of aromatic amino acids in
 solution. The formation of tyrosyl and tryptophanyl radicals
 15 upon electron transfer from the aromatic amino acids to the FQ
 triplet state as well as the formation of the $\text{FQ}^{\bullet-}$ radical anion
 was ascertained.³¹ While these results may be relevant to the
 protein photomodification induced by 6-F-quinolones, the study
 of the process with serum albumin was made difficult by their
 20 very low affinity for the protein (association constant $K_{\text{ass}} < 6 \times$
 10^2 M^{-1} for a series of 6-F-quinolones).³¹ Thus the mechanism
 for the formation of the photoadducts within protein complexes
 is still unknown. This holds for 6,8-F-quinolones also.

Differently, for the parent molecule of the 4-quinolone family, NA
 25 (Scheme 4), it has been shown that covalent photobinding to BSA
 and HSA occurs and the whole process in the drug-protein complex
 has been fairly well elucidated from a mechanistic point of view.³²
 This case study represents a sort of *whole movie* of drug photobinding
 to a protein, and has nice tutorial value. With the application of
 30 UV-absorption, fluorescence and circular dichroism (CD), the
 stoichiometry, stability constants of the order of 10^5 – 10^6 M^{-1} , and
 individual spectral features of the most stable complexes of NA^-
 with BSA and HSA were determined. Association occurs in subdo-
 mains IIA and IIIA, with the complexes having predominant 1:1
 35 stoichiometry with BSA and both 1:1 and 2:1 NA^- :SA stoichiome-
 tries with HSA. The highest affinity site is in subdomain IIIA. Laser
 flash photolysis of NA^- in buffer solution evidences the triplet
 species decaying with a lifetime of 2.1 μs . With the NA^- :SA 1:1
 complex as the predominant species absorbing the excitation light a
 40 radical pair consisting of the Tyr-O $^{\bullet}$ radical ($\lambda_{\text{max}} = 410 \text{ nm}$) and the
 $\text{NA}^{2-\bullet}$ radical ($\lambda_{\text{max}} = 640 \text{ nm}$) is detected at the end of the laser
 pulse. Actually the binding geometry of NA^- in subdomain IIIA of
 HSA shows a close interaction of the drug with Tyr411 at a distance
 of 4.24 Å in a sandwich-like structure (Fig. 4), that can justify a fast
 45 electron transfer from Tyr to $\text{NA}^{\bullet-}$. Fast deprotonation of the tyrosyl
 radical cation, according to the mechanism outlined in eqn (1),
 leads to the radical pair of Tyr-O $^{\bullet}$ and $\text{NA}^{2-\bullet}$.



50 The process, thermodynamically allowed in both the lowest
 excited singlet and triplet states of the drug, takes place within
 the laser pulse (20 ns), so the experiment does not provide
 information on the precursor state. The quantum yield of the
 radical pair is rather high (~ 0.4 – 0.5). Both Tyr-O $^{\bullet}$ and $\text{NA}^{2-\bullet}$
 55 radicals disappear by first order kinetics with a rate constant of
 $\approx 10^7 \text{ s}^{-1}$ consistent with a cage combination reaction leading

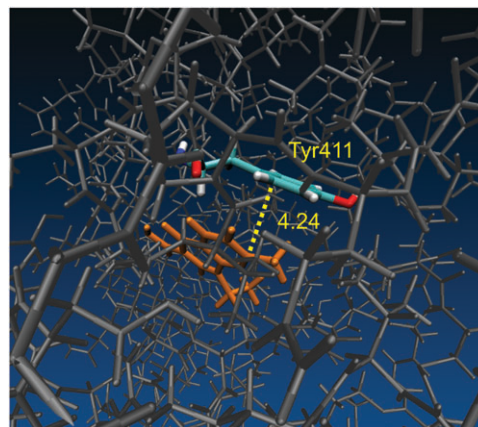
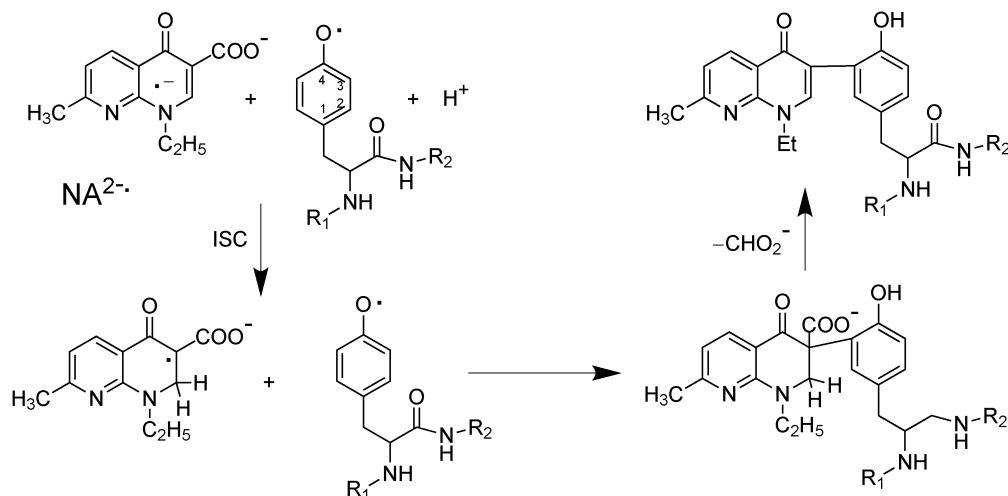


Fig. 4 Calculated structure of the 1:1 complex of nalidixate anion with HSA-subdomain IIIA. Reprinted with permission from ref. 32. Copyright (2008) American Chemical Society.

to the formation of a covalent bond. Covalent addition actually
 occurs with both HSA and BSA. Steady state photolysis with 1:1
 20 complexes as the largely prevailing species in solution reveals
 by HPLC analysis a modified protein with an enhanced drug-
 like fluorescence. A plausible mechanism for the formation of
 the adduct is outlined in Scheme 7, based on the reactivity of
 α,β -unsaturated ketones upon electron addition. The mecha-
 25 nism involves protonation of $\text{NA}^{2-\bullet}$ at C2 and addition of TyrO $^{\bullet}$
 (*ortho* position) at C3. This path is compatible with the
 observed first order kinetics of the disappearance of the radical
 pair, since the tyrosine radical cation readily deprotonates
 (eqn (1)) and the radical fragments couple in cage. The release
 30 of formate restores the conjugation in the quinolone ring of the
 adduct, so that the final modified protein exhibits a drug-like
 fluorescence.

3.2 DNA

DNA strongly differs from proteins as regards the modes of
 non-covalent ligand association, essentially because it does not
 exhibit the huge variety of conformations typical of proteins.
 DNA consists of a polymer of nucleotides linked to the back-
 40 bone of alternating deoxyribose molecules and phosphate
 groups (Fig. 6). The 3'-C of a sugar moiety is connected through
 a phosphate group to the 5'-C of the next sugar. Each sugar
 molecule is covalently linked to one of four possible bases (the
 purines, adenine and guanine, and the pyrimidines, cytosine
 45 and thymine). In doubled stranded (ds) DNA base A always
 pairs with T and G always pairs with C *via* two and three
 hydrogen bonds, respectively. The aromatic planes of the bases
 are oriented perpendicular to the helix axis. Hydrophobic sites
 locate between adjacent planes of base pairs. The backbone of
 50 the polynucleotide chain is highly charged with one negative
 charge per phosphate group balanced by positive counterions
 structurally essential for the double helix. The structural
 features of the biomolecule allow two main types of binding
 55 modes, intercalative binding between adjacent base pairs and
 minor and major groove association.



Scheme 7 The proposed path for the covalent photoaddition of NA^- to tyrosine in SA.³²

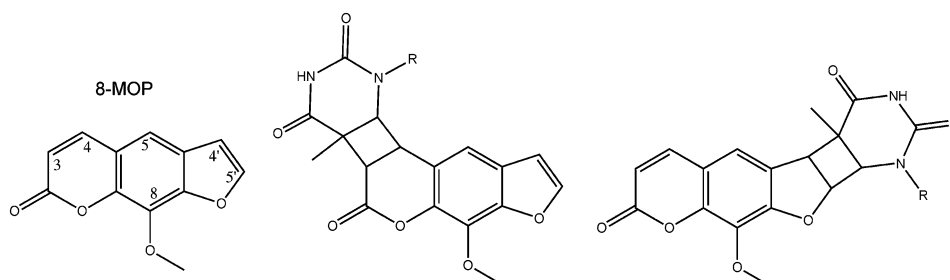
Photoexcitation of drugs in the presence of DNA may initiate chemical reactions finally leading to alkylation of the biomolecule. Clinically used drugs like psoralens¹ and 6,8-difluoroquinolones³³ are able to induce such kind of chromosomal damage in UVA-irradiated cells. Other examples of photoactivatable molecules with similar potential are platinum complexes³⁴ as well as quinone methides.³⁵ Covalent photobinding of the drug to a nucleobase and drug photosensitized dimerization of two adjacent nucleobases are examples of photoalkylation that have been studied in the presence of DNA. Not always the role of the non-covalent association of the photoalkylating agent with DNA has been explored.

The two main targets among the bases for photosensitized DNA damage are thymine and guanine: the first one has the lowest triplet energy, thus becomes the most likely energy acceptor in energy transfer processes, and the second one has the lowest oxidation potential, thus becomes the most favoured electron donor in charge transfer reactions. Note that these properties vary strongly from the individual base to the base in polynucleotide assemblies.^{36,37} Detection of DNA lesions is mostly performed by radiolabelling and subsequent gel electrophoresis. This method is often combined with the use of specific repair enzymes to reveal the type of DNA damage produced.^{8,9}

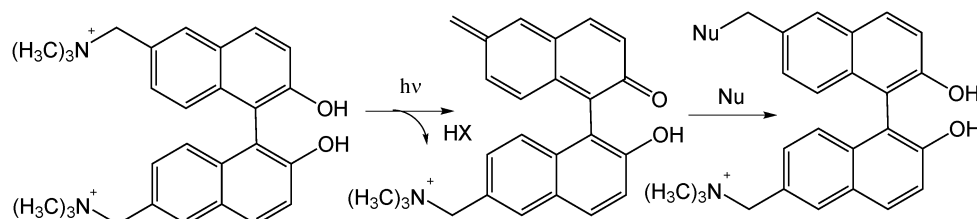
3.2.1 Furocoumarins. Furocoumarins, also known as psoralens, are a class of naturally occurring aromatic compounds with a furan ring fused to a coumarin moiety (Scheme 8). They are employed in the treatment of psoriasis and other cutaneous diseases, including cutaneous T-cell lymphoma. 8-Methoxy-psoralen (8-MOP) is one of the most used and studied derivatives.¹ The absorption spectra of psoralens are characterized by peaks at *ca.* 250 and 300 nm with a shoulder at *ca.* 340 nm extending up to 400 nm.

Two main electronic transitions are involved, one of n,π^* nature from the non-bonding orbital in the carbonyl group to the antibonding π^* orbital and the second of π,π^* nature from the bonding π orbital to the antibonding π^* orbital. The lowest energy excited states S_1 and T_1 are of π,π^* nature and are localized mainly in the benzopyrone moiety.

The main pharmacological application of psoralens relies on their ability to alkylate DNA when irradiated with UVA light, resulting in photoinduced interstrand crosslinking (ISCL). ISCL in DNA represents one of the most cytotoxic lesions as it inhibits DNA melting and, consequently, replication. Psoralens intercalate preferentially at crosslinkable 5'-TA or 5'-AT sequences. The formation constants of such complexes are of the order of 10^5 M^{-1} . Upon absorption of a UVA photon by the intercalated drug a [2+2] photocycloaddition reaction takes



Scheme 8 8-Methoxy-psoralen (8-MOP) and the thymine monoadducts on the pyrone (left) and furan (right) ring.



Scheme 9 Mechanism for generation and reaction of the quinone methide.

place, where the 5,6 double bond of the adjacent thymine adds either to a 4',5' furan double bond or to a 3,4 pyrone double bond (see Scheme 8). While a number of isomers are possible the *cis-syn* configuration is the most likely, due to the restrictions imposed by intercalation. ISCL involves formation of bis-adducts and requires sequential absorption of two photons: the first photon yields the mono-adduct on the furan ring which in turn by absorption of a second photon links *via* the pyrone ring, leading to the bis-adduct. Monoadduct formation at the pyrone ring destroys the coumarin nucleus, preventing the second photochemical event. Cytosine reacts to a lower extent. The photoreactivity of psoralens is strongly affected by the environment, and in particular by the polarity of the medium and somewhat depends on the molecular structure. There is no unambiguous evidence yet about the spin multiplicity of the excited state promoting the cycloaddition reaction. Typically both the fluorescence and the triplet quantum yields decrease in the intercalated compounds, suggesting singlet reactivity of the DNA complexes.¹

Similar to psoralens, some quinone methides (QM) generated photochemically give rise to ISCL in DNA. Recently, very promising results have been obtained for water-soluble binaphthol derivatives as QM precursors. Irradiation of DNA with 360 nm light in the presence of the binaphthol compound of Scheme 9 leads to the formation of mono and ISCL bis-adducts.³⁵ The photoexcited molecule releases the reactive QM upon excited state proton transfer. The QM adds generally to nucleophiles, and in the case of nucleotides has preference for addition to purines, in particular guanosine, in DNA.

3.2.2 Fluoroquinolones. Interaction of FQs with DNA is directly relevant to their pharmacological activity and is exemplified by the X-ray structure in Fig. 5 with ciprofloxacin (CPF) and bacterial DNA gyrase.

FQs are very effective photosensitizers of damage to cellular DNA, isolated DNA and oligonucleotides. Photogenotoxicity of FQs originates in type I and type II processes as well as triplet-triplet energy transfer photosensitization. Cyclobutane pyrimidine dimers (CPD), oxidation products of nucleobases and single strand breaks (SSB, see Section 4) are the most important lesions.³³ FQ photoinduced DNA modification depends on the FQ chemical structure affecting the drug photochemistry, the FQ affinity for DNA, the preferable site of binding, and the geometry of the FQ–DNA complex. Pyrimidine dimerization and nucleobase oxidation are the processes relevant to the formation of new covalent bonds.

In the following we first illustrate the FQ photochemistry in the presence of an individual nucleotide as a model. As anticipated, 6-monofluoroquinolones undergo heterolytic defluorination by photosubstitution at C6 and the process is mediated by longlived triplets (Scheme 6a).^{2,38} 6,8-Difluoroquinolones undergo the release of F⁻ at C8 and the resulting aryl cation (AC⁺) undergoes intramolecular cyclization (Scheme 6b). The AC⁺ species does not react with water or other *n* donors but is highly reactive with π nucleophiles to form addition products.^{28,29} A bimolecular reaction of this species with guanosine monophosphate (dGMP, $k_t > 10^9 \text{ M}^{-1} \text{ s}^{-1}$) was actually evidenced and covalent adducts were detected in photoproduct analysis (Scheme 10).³⁹ Differently, the NOR triplet was quenched by dGMP ($k_q = 7.7 \times 10^7 \text{ M}^{-1} \text{ s}^{-1}$), but photoproduct analysis did not reveal any covalent adduct. The triplet quenching

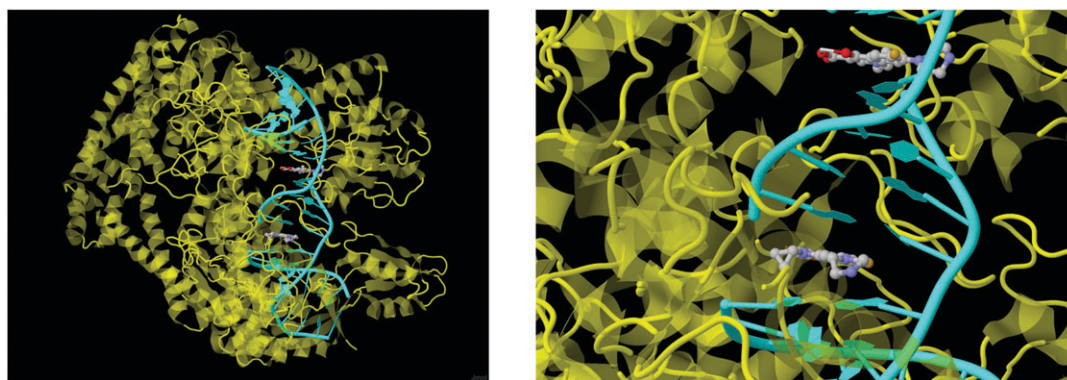
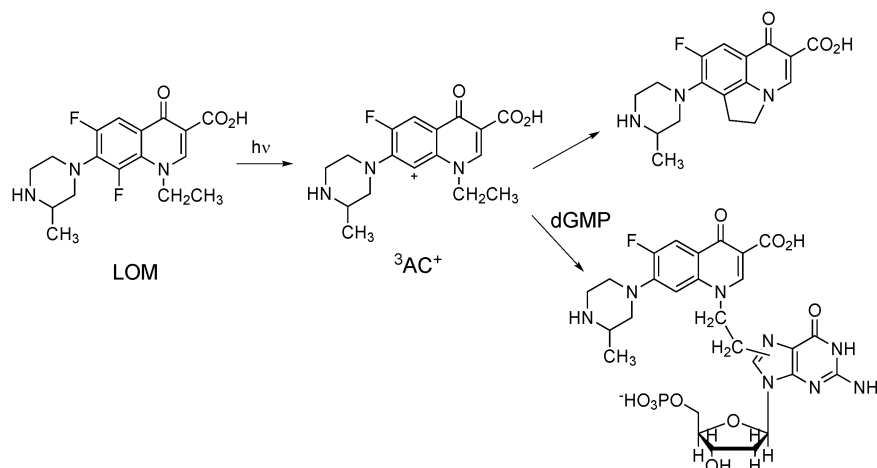


Fig. 5 Structure of the DNA gyrase complex with DNA and two ciprofloxacin (CPF) molecules, obtained from the structure with PDB code 2XCT. The right image shows a close-up view of the area indicated by the white circle.



Scheme 10 LOM intramolecular photocyclization and photoaddition to dGMP.³⁹

process is conceivably attributable to hydrogen abstraction from the sugar residue or interaction with the phosphate moiety and differs from the trapping of the aryl cation leading to addition to the heterocyclic base.³⁹

The FQ-DNA non-covalent binding modes in solution must be taken into account when searching a rationale for the intermolecular reactions in the complex. The association of FQs with calf thymus DNA is rather weak ($K_{\text{ass}} \approx 10^3 \text{ M}^{-1}$, referred to base pair).^{40,41} The likely presence of uncomplexed drug in the experiments with DNA makes interpretation of the data difficult compared to those collected with mononucleotides. The cationic form of FQs is thought to associate with DNA with the positively charged piperazinyl group bound to negatively charged DNA backbone and the neutral aromatic moiety protruding towards the DNA interior. The FQ zwitterion forms an external complex characterized by even lower association constants ($K_b \approx 10^2 \text{ M}^{-1}$) with the positively charged piperazinyl group interacting with DNA phosphate groups and the negatively charged aromatic moiety protruding into the bulk solvent.⁴⁰

The main type of FQ induced photodamage in the presence of DNA is cyclobutane pyrimidine dimer (CPD) formation.¹⁰ CPD is the result of the covalent binding of two adjacent pyrimidine bases, one in the excited state and the other in the ground state.⁹

UVA photosensitized CPD formation in DNA is typically the result of triplet-triplet energy transfer from an exogenous photosensitizer to a thymine, the nucleobase with the lowest triplet energy ($E_T = 310 \text{ kJ mol}^{-1}$ for dTMP) (Fig. 6). The reaction is a [2+2] photocycloaddition of ³dThy with an adjacent dThy in the ground state (Scheme 11). CPD formation can be sensitized by FQs with an E_T threshold of 265–269 kJ mol^{-1} .⁹ This result implicates that base stacking and base pairing decrease the thymine triplet energy from 310 kJ mol^{-1} down to *ca.* 267 kJ mol^{-1} making energy transfer from ³FQ feasible.³⁶ CPD formation most efficiently occurs with 6-monofluoro derivatives that have longlived triplet states ($\tau_T \geq 1 \mu\text{s}$) but has also been observed with 6,8-difluoro derivatives,³³ in spite of their much shorter triplet lifetime ($\tau_T \approx 40 \text{ ns}$).^{28,29} Note that this mechanism does

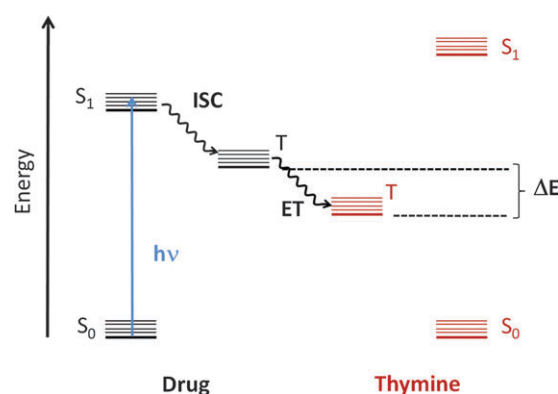
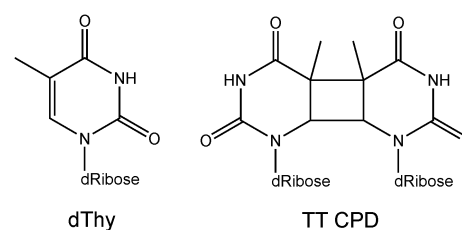


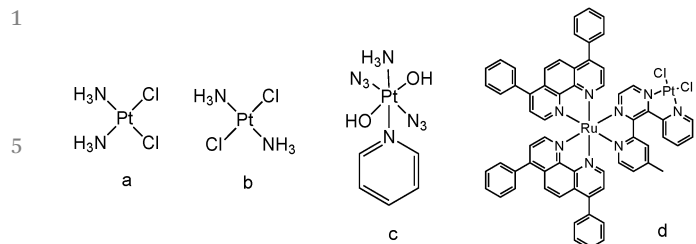
Fig. 6 Drug mediated conversion of UVA excitation energy to triplet thymine (ET, energy transfer, ISC, intersystem crossing).

not necessarily require the formation of a specific drug-DNA complex. In the case of 6-monofluoro derivatives the long triplet lifetimes can allow efficient energy transfer also in collisional encounter complexes.

Photooxidation of DNA in the presence of the FQs takes place through both type I and type II processes, the latter requiring singlet oxygen. We will recall these processes in Section 4.1.1 on FQ photoinduced DNA cleavage. As expected the type II mechanism is mainly operative in 6-monofluoro FQs.¹⁰ No transients attributable to any FQ-DNA complex have ever been observed, so the mechanisms for type I



Scheme 11 Deoxythymidine (dThy) and the cyclobutane pyrimidine dimer of two dThy (TT CPD).



Scheme 12 (a) *cis*-Pt(NH₃)₂Cl₂, (b) *trans*-Pt(NH₃)₂Cl₂, (c) all-*trans*-[Pt(N₃)₂(OH)₂(Py)₂], (d) [(Ph₂phen)₂Ru(dpp)PtCl₂]²⁺.

photooxidation of DNA in the supramolecular species have still to be clarified. Several paths are possible: (i) electron transfer within the excited complex, followed by F⁻ release from the FQ radical anion, or (ii) only in 6,8-difluoro derivatives, electron transfer to the aryl cation AC⁺, arising from heterolytic photodefluorination of the drug at C8.^{2,28} The electron is transferred preferentially from the guanine base which has the lowest oxidation potential. As to mechanism (i) electron transfer in the complex could occur either in the FQ excited singlet state, competing with intersystem crossing, or in the FQ triplet state. Type I photooxidation of DNA by FQs could mediate covalent binding of FQ to DNA. The latter process, however, has not been proved up to now. In the case of 6,8-difluoroquinolones nucleobase oxidation by the AC⁺ cation has been suggested as an alternative path for the formation of thymine dimers.²⁸

3.2.3 Metal coordination compounds. Metal coordination compounds are interesting agents for biomedical applications and some of them hold promising features for DNA photoalkylation.³⁴ In the following we focus on photoactivatable Pt compounds with potential for application in photochemotherapy. Their story starts with a very simple compound [*cis*-Pt(NH₃)₂Cl₂], known as *cis*-platin (Scheme 12).

Platinum complexes such as cisplatin, carboplatin and oxaliplatin are very intensively used as drugs in chemotherapy of specific tumors in spite of their severe side effects. These drugs act through thermal covalent addition to DNA, which causes a distortion in the biomolecule structure that ultimately leads to disruption of cellular transcription and cell death. The covalent binding of cisplatin to DNA involves thermal substitution of Cl⁻ by water molecules to form the [*cis*-PtCl(H₂O)(NH₃)₂]⁺ and [*cis*-Pt(NH₃)₂(OH₂)₂]²⁺ intermediates. The latter cations upon reduction bind to the N7 of guanine, finally leading to *intrastrand* crosslinks between neighboring dGuo units. The *cis* geometrical arrangement of the chloride ligands is crucial for the achievement of the final bis-adducts. Recently, the possibility emerged to employ photochemical methods to trigger covalent DNA binding of platinum complexes.³⁴ *trans*-Pt(IV) complexes, completely inert *via* purely thermal pathways, can become active upon irradiation with UVA light.⁴² For example, the octahedral complex all-*trans*-[Pt(N₃)₂(OH)₂(Py)₂] (Scheme 12c) in the presence of dGMP undergoes photochemical reduction and azide substitution yielding a *trans*-azido-dGMP mono-adduct and upon subsequent substitution of the second azide the *trans*-[Pt(Py)₂(dGMP)₂] adduct. In cancer cell cultures this complex

exhibits 10-fold enhanced genotoxic activity, when activated with visible light (420 nm), compared to cisplatin.

A new mechanism was recently proposed for the photobinding of the [(Ph₂phen)₂Ru(dpp)PtCl₂]²⁺ complex (Scheme 12d) to DNA. Excitation with visible light (≥590 nm) of the MLCT transition in Ru(II) increases electron density on dpp, decreasing the acidity of the attached Pt center. This facilitates labilization of the chloride coordination bonds and hydrolysis, leading to efficient DNA binding. This example illustrates the role of the supramolecular interactions in the complex in activating the reactivity at the Pt site with a photon of much lower energy than that required to directly excite the Pt-associated electronic transitions.⁴³

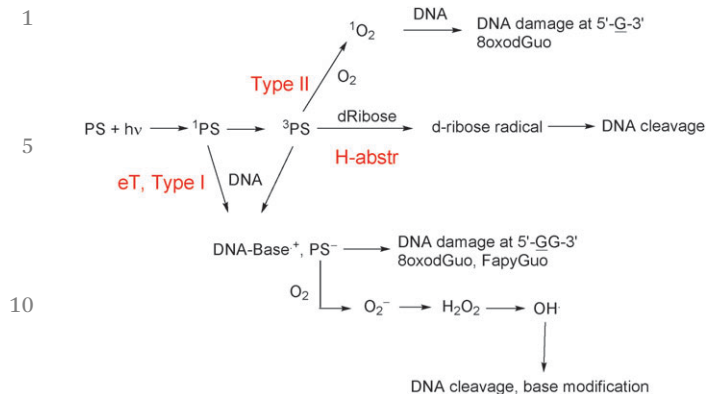
4. Drug photosensitized cleavage of covalent bonds

Above we have discussed how irradiation of drug–biomolecule systems can lead to formation of covalent bonds in the biomolecule. Another phenomenon that can take place is the cleavage of existing covalent bonds.^{8,44} Such processes may be at the origin of severe light-induced disorders in living systems, but can also be exploited in medicine and biotechnology. From a mechanistic point of view the photocleavage of a biomolecule induced by a photosensitizer typically involves an initial photooxidative process. The formation of non-covalent complexes is not a necessary requisite. In this context it is important to distinguish between DNA and proteins exhibiting a different behavior due to their specific structure.

4.1 DNA

Once in the electronically excited state, the photosensitizer can react directly with DNA causing an immediate scission of the nucleic acid chain. In reality, very few compounds act through this mechanism.⁴⁴ The vast majority of compounds capable of DNA photocleavage are those whose excited states can *initiate* a series of chemical reactions which *ultimately* lead to nucleic acid cleavage.^{8,44} Indeed, photosensitizing agents generate photochemically reactive intermediates, such as radicals, carbenes, and carbocations, which, in turn, trigger cleavage of the nucleic acid. Some photosensitizing compounds instead do not cause direct cleavage, but inflict other types of damage on the DNA making it more susceptible to cleavage in a secondary process. When generating diffusible reactive species a photocleaving agent need not even bind to the nucleic acid in order to be effective. Generally, the nature of the oxidative pathways at the origin of DNA cleavage depends on the location of the photosensitizer and on the properties of the excited state of the photosensitizer. Studies in solution in the presence of single nucleobases and DNA aimed at determining the nature of the stable photoproducts contributed to elucidate the pathways that may be operative in the cells. We briefly recall the mechanisms relevant to these phenomena in Scheme 13.

(a) *Oxidative pathway involving the hydroxyl radical (•OH).* The oxidative pathway involving the hydroxyl radical has to be

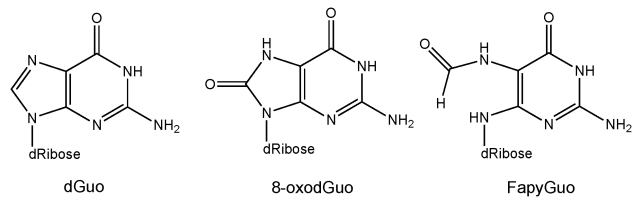


Scheme 13 Main photosensitized oxidative pathways at the origin of DNA cleavage (eT, electron transfer; PS, photosensitizer; H-abstr, H-abstraction).

considered in this context because it is indirectly initiated by a photochemical step. $\bullet\text{OH}$ results from the fate of the far less reactive $\text{O}_2^{\bullet-}$ species, produced in type I processes by the reaction of the photosensitizer radical anion with molecular oxygen. $\text{O}_2^{\bullet-}$ can be converted into hydrogen peroxide which in turn is the precursor of $\bullet\text{OH}$ in the presence of reduced metal ions like Fe^{2+} or Cu^+ . $\bullet\text{OH}$ reactions do not exhibit target specificity and occur with all components of DNA at diffusion-controlled rates. $\bullet\text{OH}$ radicals are known to attack the sugar backbone and cause cleavage through hydrogen abstraction.

(b) *Cleavage at the sugar backbone upon H-abstraction.* Direct oxidation of deoxyribose *via* hydrogen abstraction from the sugar furanose ring is another mechanism involving the excited photosensitizer.⁴⁵ The resulting sugar radicals can decompose by a variety of pathways to yield DNA fragments. The hydrogen atoms on carbons C1, C3, C4, and C5 are all targets for H-abstraction due to the presence of heteroatoms at the α -positions. The presence of identical deoxyribose residues along the DNA chain makes cleavage by H-abstraction to be inherently nonselective with respect to the sequence. A photocleaver can be highly selective if it only binds to one or a few sequences within the DNA target. Control of the sequence selectivity by varying the chemical structure of the photocleaver is a key point in the design of new DNA cleavage agents.

(c) *One-electron oxidation of DNA.* As we have mentioned, photosensitizers which bind non-covalently to DNA can, in their excited state, cause one-electron oxidation of a DNA base (type I mechanism). The efficiency of this reaction is determined by the oxidation potential and the reactivity of the four bases which can vary over a wide range, with guanine being the most easily oxidized. It is important to keep in mind that a charge migration can occur along the DNA chain and the base radical cation can be finally trapped by an irreversible reaction away from the site of generation. Trapping most frequently occurs at GG sites because of their significantly lower oxidation potential and higher reactivity with respect to “isolated” G.³⁷ Thus, regardless of the binding site of the photosensitizer, photochemical damage mainly involves guanine. The guanine



Scheme 14 dGuo and two oxidation products, 8-oxodGuo and FapyGuo.

radical cation ($\text{Gua}^{\bullet+}$) may undergo subsequent conversion to 8-oxoGuo and 2,6-diamino-4-hydroxy-5-formamidopyrimidine (FapyGuo) (Scheme 14). Note that this reaction mechanism does not directly cause DNA cleavage, but generates the so-called easily cleavable alkali labile sites.

(d) *Singlet oxygen-mediated oxidation of guanine in DNA.* $^1\text{O}_2$ (type II mechanism) exhibits a strong reactivity with double bonds giving rise to dioxetanes, endoperoxides or ene-oxidation products. The unique target among DNA components is guanine which is converted into a 4,8-endoperoxide through Diels Alder [4+2] photocycloaddition reaction. The endoperoxide quantitatively rearranges within ds-DNA into 8-hydroxyperoxyguanine that is further reduced into 8-oxoGuo, the exclusive $^1\text{O}_2$ oxidation product. It is now established that $^1\text{O}_2$ has no ability to cleave directly the DNA backbone, but as said before, this oxidative damage makes the DNA more susceptible to strand cleavage.

In the following we focus on photosensitizing drugs that lead to photocleavage of DNA by type I mechanisms. Generally, photocleavage experiments are carried out on supercoiled circular plasmid DNA, a very useful tool to study different types of DNA damage. Single-strand breaks (SSB) result in the conversion of the circular supercoiled form (also called form I) into the circular relaxed form (or form II) and can be observed directly by means of gel electrophoresis of irradiated solutions. Often DNA photocleavage is used as an analytical tool when photodamage of the nucleic acid occurs without immediate strand break and only a secondary treatment, such as incubation with hot piperidine or aniline, produces strand breaks, fully revealing sites and the extent of oxidative damage.

4.1.1 Fluoroquinolones. Almost all the compounds of this class induce photocleavage of DNA.^{10,27} Several reaction mechanisms have been invoked. Martinez *et al.*⁴⁶ evaluated the photocleaving potential of several (fluoro)quinolones, namely LOM, fleroxacin (FLX), ENX, NOR, and NA, with supercoiled plasmid pBR322 DNA. They performed irradiation experiments in both the presence and absence of oxygen, in conditions where a significant amount of free drug was also present in solution. They found that the two 6,8-difluoroquinolones, LOM and FLX, are 10-fold more efficient photocleavers in anaerobic conditions than NOR, ENX and NA. Although this does not necessarily mean that ds-DNA in the cell will be cleaved under the same conditions, LOM and FLX, the two most photogenotoxic fluoroquinolones, did cause the largest amount of strand breaks in plasmid DNA. The authors did not propose a reaction mechanism, but hypothesized the photoinduced formation of a “carbene” upon heterolytic defluorination, capable of breaking DNA. No transients have been detected up to now in LOM complexed to

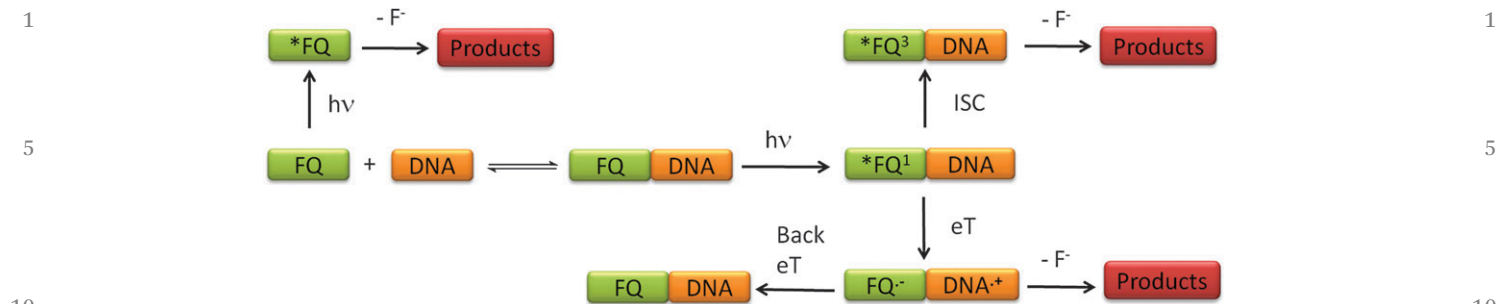


Fig. 7 Type I photosensitized paths, independent of oxygen, invoked to rationalize DNA damage by ENX and LOM.

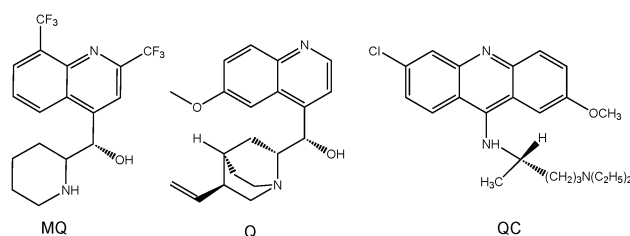
ct-DNA to support this view.⁴⁰ Other authors have compared base photodegradation products of dGuo, isolated DNA and cellular DNA with LOM, ENX, or NOR upon exposure to UVA light in the presence of oxygen.¹⁰ It was shown that NOR and, to a lesser extent, ENX act *via* $^1\text{O}_2$ oxidation, whereas LOM and, in part, ENX act *via* one-electron oxidation of purine and pyrimidine bases. Of the three FQs NOR was found to be the most efficient in inducing strand breaks. Note however that for all the investigated FQs the extent of oxidatively mediated damage was relatively low and the formation of CPD represented the major photodamage in both isolated and cellular DNA. The above results show how biological data relevant to FQ-induced DNA photocleavage from different laboratories may be contradictory. An important parameter that can be responsible of the discrepancies is the actual extent of non-covalent association of the drug with the biomolecule in the experiments.

The role of drug binding to ct-DNA was comparatively investigated with LOM and ENX, in neutral PB at various concentrations.⁴⁰ Among the 6-monofluoroquinolones ENX is one of the most efficient type I DNA photosensitizers. Binding to ct-DNA occurs with $K_{\text{ass}} = 3.2 \times 10^3 \text{ M}^{-1}$. The quantum yield for photocleavage of plasmid pBR322 DNA investigated in anaerobic conditions is twice that in aerobic conditions.⁴⁷ In diluted PB (10^{-3} M) the photodefluorination quantum yield progressively decreases in the presence of increasing amounts of ct-DNA, while the ENX triplet is generated with lower efficiency, but with unchanged lifetime. These data show the prominent role of the triplet state in the ENX photodefluorination process and reflect the formation of an essentially unreactive ENX-DNA complex. The observed amount of released fluoride was attributed to the unbound fraction of the drug. Increasing concentrations of phosphate ions in the buffer are able to displace the ENX molecules from the DNA interior exposing them in complexes of lower stability ($K_{\text{ass}} \approx 4 \times 10^2 \text{ M}^{-1}$). While the $\text{HPO}_4^{2-}/\text{HPO}_4^-$ ions of the buffer are able to reduce the triplet state of ENX (most likely in zwitterionic form in the external complex), thereby driving the F^- detachment,² direct triplet state reduction by the phosphate ions of the DNA backbone was excluded.⁴⁰ In the case of LOM in conditions of partial association with DNA ($K_{\text{ass}} = 1.3 \times 10^3 \text{ M}^{-1}$) the photodefluorination quantum yield is unaffected, *i.e.* the release of fluoride does not appreciably modify the excited complex.⁴⁰ This was explained either by unperturbed conversion of $^1\text{FQ}^*$ to

the triplet state followed by heterolytic defluorination yielding the AC^+ species or by one-electron redox process within the singlet excited complex, followed by defluorination of the radical anion $\text{FQ}^{\bullet-}$, as described in Section 3.2.2. Type I oxidation of a nucleobase in both cases generates radicals finally leading to strand breaks. Fig. 7 resumes the main type I photosensitized paths, independent of oxygen, invoked to rationalize DNA damage by ENX and LOM.

As a final remark of this section it is worth underlining that photosensitized cleavage of DNA by FQs can be initiated by a photochemical act occurring either in the complexed drug, *i.e.* “within” the biomolecular frame, or in the free drug. In the latter case the photogenerated reactive intermediates diffuse in the buffer attacking and damaging the biomolecule. Electron transfer to FQ^* from salt ions in the buffer can contribute to the formation of radicals which participate in the damaging reactions. Thus when comparing photochemical/photobiological data from different laboratories the key factors relevant to the experimental conditions to be compared are not only the presence or absence of oxygen and the extent of drug-biomolecule association, but also the nature and the concentration of the buffer.

4.1.2 Quinine-like antimalarials. The antimalarial drugs quinine, mefloquine and quinacrine (Scheme 15) exhibit a DNA photocleavage power that was interpreted in the light of the affinity of these drugs for DNA.⁴⁸ Absorption and emission spectroscopy as well as linear dichroism evidenced that these derivatives bind to the macromolecule with good binding constants ($\text{p}K_{\text{a}}$ values of *ca.* 4.6–5.0). The absorption characteristics of the drugs change markedly upon addition of DNA and their fluorescence was quenched with rate constants higher than those of diffusion indicating static quenching in the drug-DNA complex. The predominant binding mode is intercalation into the double helix. The DNA photocleavage properties of



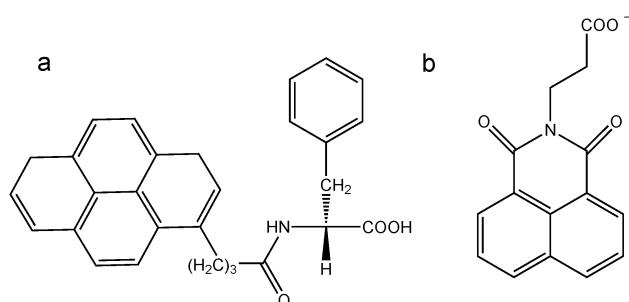
Scheme 15 Mefloquine (MQ), quinine (Q) and quinacrine (QC).

1 antimalarials were investigated using pBR322 plasmid DNA as
 a model, at different [drug][DNA] ratios. The authors investi-
 5 gated the system for the presence of frank breaks due to direct
 drug photosensitized cleavage. The results indicate that Q, MQ
 and QC are able to induce frank strand breaks to a different
 extent as well as significant oxidative DNA photodamage
 10 inflicted on both purines and pyrimidines as revealed by means
 of enzyme treatment. The highest levels of frank strand breaks
 have been found for Q, and this effect is even more evident in
 anaerobic conditions. The photocleavage in the absence of
 oxygen has been related to photoionization in the singlet
 excited state for Q and QC and in the triplet excited state for
 MQ, generating the radical cation capable of oxidizing and
 finally cleaving the DNA strand.

4.2 Proteins

Protein photocleavage by drugs is much less documented
 compared to other types of drug photoinduced damage in
 20 proteins. In this section we therefore focus on specific cleavage
 of proteins by small molecules, an important tool in molecular
 biology to investigate protein structure and biomolecular inter-
 actions. By means of this method information on the exposure
 of residues of membrane-bound proteins, design of new ther-
 25 apeutic agents or fragmentation of large proteins for sequen-
 cing can be obtained. Generally type I photooxidation is the
 initiating process and radical species are generated in the
 system. Biomolecular fragmentation results from reactions of
 these radicals. Frequently tyrosine and tryptophan are involved,
 30 representing major sites for stable radical trapping. The affinity
 of the photocleaving agent for the protein substrate is not
 always a key point, as will result in the following.

Very appealing tools are the so-called “photochemical pro-
 35 teases”, *i.e.* protein cleaving agents characterized by intense
 absorption in the UVA, Vis or near IR region, long-lived excited
 states useful to initiate photoreactions, and high affinities for
 selected sites of proteins. Such features are all present in a
 series of pyrenyl-derivatized peptides which also bear a fluor-
 40 escent chromophore to probe the environment.⁴⁹ The L and
 R enantiomers of *N*-(l-phenylalanine)-4-(1-pyrene)butyramide
 (Py-Phe, Scheme 16) bind to lysozyme with similar binding
 constants of 10^5 M^{-1} and the absorption spectra point to a
 binding site with large solvent exposure. Differently R-Py-Phe
 and L-Py-Phe bind to BSA with binding constants of 5×10^5 and



Scheme 16 Proteases Py-Phe (a) and NI-ala (b).

$7 \times 10^7 \text{ M}^{-1}$, respectively, evidencing a marked stereodiffer-
 entiation. Red shifted absorption spectra, CD and fluorescence
 of Py-Phe within BSA suggest a different hydrophobic environ-
 ment for the two enantiomers. Irradiation of L-Py-Phe with
 344 nm light, in the presence of the electron acceptor Co(III)
 5 hexamine (CoHA), causes site-specific lysozyme and BSA cleav-
 age, with quantum yields of 0.26 and 0.0021, respectively.
 Cleavage does not proceed in the dark or in the absence of Py-L-
 Phe or CoHA. In this case lower binding affinity does not
 negatively influence the photocleavage efficiency. The lower
 10 photocleavage yield for BSA is attributed to better protection
 from the Co(III) complex of Py-L-Phe offered by the protein.
 Photoproduct analysis reveals a single cleavage site for both
 enantiomers between Trp 108 and Val109 and Leu346 and
 Arg347, for lysozyme and BSA, respectively. Stereodifferentiation
 in binding to BSA of the two Py-Phe enantiomers does not
 translate into a change in cleavage-site specificity. Laser flash
 photolysis of a mixture of protein, Py-Phe, and CoHA reveals two
 20 transients, triplet Py-Phe with an absorption maximum at
 420 nm and the pyrenyl cation radical with absorption centered
 at 460 nm. The latter results from quenching of the singlet excited
 state of Py-Phe by CoHA. Upon deprotonation of the pyrenyl cation
 radical H-atom abstraction by the neutral pyrenyl radical from the
 side chains of the amino acid residues present at the probe binding
 site was proposed to mediate the photocleavage. Molecular model-
 25 ing of lysozyme actually shows that the side chains of Trp108 and
 Val109 are exposed into the active site cavity.

Other photoactive organic compounds that have shown protein
 cleavage capability are naphthaleneimides. *N*-(2-ethanoic acid)-1,8-
 naphthalimide (NI-ala, Scheme 16) induces photocleavage and
 photocrosslinking of lysozyme.⁵⁰ Cleavage was attributed to redox
 processes between the NI-ala triplet and lysozyme amino acids
 forming longlived radicals in the system. Singlet state quenching
 does not give rise to longlived redox intermediates and was believed
 35 to be not relevant to oxidative damage pathways. Some aspects
 of the mechanism were elucidated by experiments with aromatic
 amino acids, lysozyme and BSA. In the presence of tryptophan,
 tyrosine and lysozyme chemical quenching of the NI-ala triplet
 leads to the formation of longlived NI-ala^{•-} and Trp(-H)[•] radicals,
 detected by nanosecond transient spectroscopy.

Despite that the NI-ala triplet was quenched by BSA too, no
 radicals were detected. It was concluded that the initial redox
 reaction is followed by deprotonation of the amino acid radical
 cation and separation of the radical pair. The exposure of the
 reaction site in the protein controls the yield of NI-ala^{•-}
 45 through the competition between deprotonation and back
 electron transfer, the latter favoured in BSA. Lysozyme with
 respect to BSA has more Trp and Tyr residues exposed to
 solvent and can therefore offer more sites where effective
 photocleavage can take place.

5. Concluding remarks

In this tutorial review we have examined the main mechanisms
 for the photochemical modification of protein and DNA, with

1 formation of new covalent bonds or cleavage of existing bonds,
 upon light absorption in drug–biomolecule supramolecular
 complexes. This topic has relevance to drug mediated
 photosensitized adverse effects and various forms of photo-
 5 chemotherapy. It also inspires scientists looking for innovation
 in nanomedicine, biotechnology and molecular biology.
 Indeed, new photoactivatable ligands for photoaffinity label-
 ling or photorelease of caged compounds are being explored as
 tools in drug development, and also photochemical proteases
 10 and nucleases are being used for the control of the activity of
 genes and proteins and the investigation of their structure and
 interactions. The use of light as a reagent for biomolecule
 modification has indeed several advantages, because reactions
 triggered and sustained with light allow a precise control of
 15 reaction initiation and termination and possess better features
 in terms of selectivity and effectiveness in mild conditions.
 Focusing on selected drugs or potential drugs we have
 evidenced how the supramolecular architecture of the drug–
 biomolecule complex can control the final photochemical out-
 20 come. We have also shown that only a careful study of the drug
 affinity for the biomolecule, concomitant to the investigation of
 the drug photochemistry, can allow understanding of the
 photoreactions in a drug–biomolecule complex. Extrapolation
 of the results obtained to the cellular environment is not
 25 without risks and needs further investigations. Indeed a lot of
 other actors go on stage in biological systems.

Acknowledgements

30 We acknowledge the FP7 PEOPLE-ITN project no. 237962-
 CYCLON and the AIRC project “Multimodal cancer therapy
 implemented with functionalized photoactivable nanoparticles”
 for partial support of our research.

References

- 1 N. Kitamura, S. Kohtani and R. Nakagaki, *J. Photochem. Photobiol., C*, 2005, **6**, 168–185.
- 2 A. Albini and S. Monti, *Chem. Soc. Rev.*, 2003, **32**, 238–250.
- 3 S. Monti and S. Sortino, *Chem. Soc. Rev.*, 2002, **31**, 287–300.
- 4 M. C. Cuquerella, V. Lhiaubet-Vallet, J. Cadet and M. A. Miranda, *Acc. Chem. Res.*, 2012, **45**, 1558–1570.
- 5 V. Lhiaubet-Vallet and M. A. Miranda, *Pure Appl. Chem.*, 2006, **78**, 2277–2286.
- 6 I. Andreu, C. Mayorga and M. A. Miranda, *Curr. Opin. Allergy Clin. Immunol.*, 2010, **10**, 303–308.
- 7 D. Dolmans, D. Fukumura and R. K. Jain, *Nat. Rev. Cancer*, 2003, **3**, 380–387.
- 8 J. Cadet, S. Mouret, J.-L. Ravanat and T. Douki, *Photochem. Photobiol.*, 2012, **88**, 1048–1065.
- 9 M. C. Cuquerella, V. Lhiaubet-Vallet, F. Bosca and M. A. Miranda, *Chem. Sci.*, 2011, **2**, 1219–1232.
- 10 S. Sauvaigo, T. Douki, F. Odin, S. Caillat, J. L. Ravanat and J. Cadet, *Photochem. Photobiol.*, 2001, **73**, 230–237.
- 11 S. Sortino, *J. Mater. Chem.*, 2012, **22**, 301–318.
- 12 X. M. He and D. C. Carter, *Nature*, 1992, **358**, 209–215.
- 13 L. Deschamps-Labat, F. P  hourcq, M. Jagou and B. Bannwarth, *J. Pharm. Biomed. Anal.*, 1997, **16**, 223–229; T. Maruyama, C. C. Lin, K. Yamasaki, T. Miyoshi, T. Imai, M. Yamasaki and M. Otagiri, *Biochem. Pharmacol.*, 1993, **45**, 1017–1026; S. Monti, F. Manoli, S. Sortino, R. Morrone and G. Nicolosi, *Phys. Chem. Chem. Phys.*, 2005, **7**, 4002–4008.
- 14 S. Monti, I. Manet, F. Manoli, R. Morrone, G. Nicolosi and S. Sortino, *Photochem. Photobiol.*, 2006, **82**, 13–19.
- 15 S. Monti, I. Manet, F. Manoli and S. Sortino, *Photochem. Photobiol. Sci.*, 2007, **6**, 462–470.
- 16 F. Bosca, M. L. Marin and M. A. Miranda, *Photochem. Photobiol.*, 2001, **74**, 637–655; J. Moser, A. Hye, W. W. Lovell, L. K. Earl, J. V. Castell and M. A. Miranda, *Toxicol. In Vitro*, 2001, **15**, 333–337; G. Cosa, *Pure Appl. Chem.*, 2004, **76**, 263–275.
- 17 M. A. Miranda, *Pure Appl. Chem.*, 2001, **73**, 481–486.
- 18 A. Lahoz, D. Hernandez, M. A. Miranda, J. Perez-Prieto, I. M. Morera and J. V. Castell, *Chem. Res. Toxicol.*, 2001, **14**, 1486–1491.
- 19 G. Marconi, E. Mezzina, I. Manet, F. Manoli, B. Zambelli and S. Monti, *Photochem. Photobiol. Sci.*, 2011, **10**, 48–59.
- 20 G. Cosa, M. Lukeman and J. C. Scaiano, *Acc. Chem. Res.*, 2009, **42**, 599–607.
- 21 M.-D. Li, J. Ma, T. Su, M. Liu, L. Yu and D. L. Phillips, *J. Phys. Chem. B*, 2012, **116**, 5882–5887.
- 22 M.-D. Li, C. S. Yeung, X. Guan, J. Ma, W. Li, C. Ma and D. L. Phillips, *Chem.–Eur. J.*, 2011, **17**, 10935–10950; T. Suzuki, T. Okita, Y. Osanai and T. Ichimura, *J. Phys. Chem. B*, 2008, **112**, 15212–15216.
- 23 T. Suzuki, M. Shinoda, Y. Osanai and T. Isozaki, *J. Phys. Chem. B*, 2013, **117**, 9662–9668; M. Shinoda, T. Isozaki and T. Suzuki, *Photochem. Photobiol.*, 2013.
- 24 S. Monti, I. Manet and G. Marconi, *Phys. Chem. Chem. Phys.*, 2011, **13**, 20893–20905.
- 25 K. Kaneko, V. T. G. Chuang, T. Ito, A. Suenaga, H. Watanabe, T. Maruyama and M. Otagiri, *Die Pharmazie*, 2012, **67**, 414–418.
- 26 T. Su, J. Ma, M.-D. Li, X. Guan, L. Yu and D. L. Phillips, *J. Phys. Chem. B*, 2013, **117**, 811–824.
- 27 G. de Guidi, G. Bracchitta and A. Catalfo, *Photochem. Photobiol.*, 2011, **87**, 1214–1229.
- 28 M. Freccero, E. Fasani, M. Mella, I. Manet, S. Monti and A. Albini, *Chem.–Eur. J.*, 2008, **14**, 653–663.
- 29 E. Fasani, S. Monti, I. Manet, F. Tilocca, L. Pretali, M. Mella and A. Albini, *Org. Lett.*, 2009, **11**, 1875–1878.
- 30 S. Soldevila and F. Bosca, *Org. Lett.*, 2012, **14**, 3940–3943.
- 31 F. Bosca, *J. Phys. Chem. B*, 2012, **116**, 3504–3511.
- 32 S. Monti, I. Manet, F. Manoli, M. L. Capobianco and G. Marconi, *J. Phys. Chem. B*, 2008, **112**, 5742–5754.
- 33 V. Lhiaubet-Vallet, F. Bosca and M. A. Miranda, *Photochem. Photobiol.*, 2009, **85**, 861–868.
- 34 D. Crespy, K. Landfester, U. S. Schubert and A. Schiller, *Chem. Commun.*, 2010, **46**, 6651–6662.
- 35 D. Verga, M. Nadai, F. Doria, C. Percivalle, M. Di Antonio, M. Palumbo, S. N. Richter and M. Freccero, *J. Am. Chem. Soc.*, 2010, **132**, 14625–14637.

- 1 36 F. Bosca, V. Lhiaubet-Vallet, M. C. Cuquerella, J. V. Castell and M. A. Miranda, *J. Am. Chem. Soc.*, 2006, **128**, 6318–6319.
- 37 S. Kanvah, J. Joseph, G. B. Schuster, R. N. Barnett, C. L. Cleveland and U. Landman, *Acc. Chem. Res.*, 2010, **43**, 280–287.
- 5 38 M. C. Cuquerella, F. Bosca and M. A. Miranda, *J. Org. Chem.*, 2004, **69**, 7256–7261; F. Lorenzo, S. Navaratnam and N. S. Allen, *J. Am. Chem. Soc.*, 2008, **130**, 12238–+.
- Q7** 39 E. Fasani, I. Manet, M. L. Capobianco, S. Monti, L. Pretali and A. Albini, *Org. Biomol. Chem.*, 2010, **8**, 3621–3623.
- 10 40 S. Sortino and G. Condorelli, *New J. Chem.*, 2002, **26**, 250–258.
- 41 G. S. Son, J. A. Yeo, M. S. Kim, S. K. Kim, A. Holmen, B. Akerman and B. Norden, *J. Am. Chem. Soc.*, 1998, **120**, 6451–6457.
- 15 42 N. J. Farrer, J. A. Woods, L. Salassa, Y. Zhao, K. S. Robinson, G. Clarkson, F. S. Mackay and P. J. Sadler, *Angew. Chem., Int. Ed.*, 2010, **49**, 8905–8908.
- 20 43 S. L. H. Higgins, A. J. Tucker, B. S. J. Winkel and K. J. Brewer, *Chem. Commun.*, 2012, **48**, 67–69.
- 44 B. Armitage, *Chem. Rev.*, 1998, **98**, 1171–1200.
- 45 D. T. Breslin, J. E. Coury, J. R. Anderson, L. McFail-Isom, Y. Kan, L. D. Williams, L. A. Bottomley and G. B. Schuster, *J. Am. Chem. Soc.*, 1997, **119**, 5043–5044.
- 5 46 L. Martinez and C. F. Chignell, *J. Photochem. Photobiol., B*, 1998, **45**, 51–59.
- 47 S. Sortino, G. Condorelli, G. De Guidi and S. Giuffrida, *Photochem. Photobiol.*, 1998, **68**, 652–659.
- 10 48 G. G. Aloisi, M. Amelia, A. Barbafina, L. Latterini, F. Elisei, F. dall'Acqua, D. Vedaldi, A. Faccio and G. Viola, *Photochem. Photobiol.*, 2007, **83**, 664–674.
- 49 C. V. Kumar, A. Buranaprapuk, H. C. Sze, S. Jockusch and N. J. Turro, *Proc. Natl. Acad. Sci. U. S. A.*, 2002, **99**, 5810–5815.
- 15 50 B. Abraham and L. A. Kelly, *J. Phys. Chem. B*, 2003, **107**, 12534–12541.
- 20
- 25
- 30
- 35
- 40
- 45
- 50
- 55